Chemistry & Biology, Vol. 11, 1147–1156, August, 2004, ©2004 Elsevier Ltd. All rights reserved. DOI 10.1016/j.chembiol.2004.05.023

A Structural Basis for the Species-Specific Antagonism of 26,23-Lactones on Vitamin D Signaling

Mikael Peräkylä,[1,3] Ferdinand Molnár,[2,3] and Carsten Carlberg[2,*]
[1]Department of Chemistry
[2]Department of Biochemistry
University of Kuopio
FIN-70211 Kuopio
Finland

Summary

The 26,23-lactone derivative of 1α,25-dihydroxyvitamin D_3, TEI-9647, is a partial antagonist of the of human vitamin D receptor (VDR). However, we found that TEI-9647 in rat cells behaves as a weak VDR agonist. This behavior could be mimicked in human cells by the double mutagenesis of human VDR (specifically C403S and C410N). The increased agonistic action of TEI-9647 correlates to a gain in the interaction of the VDR with coactivator protein and a decreased stabilization of the antagonistic conformation of the receptor. Molecular dynamics simulations indicated that TEI-9647 acts as antagonist of human VDR by reducing the stability of helix 12 of the ligand binding domain. In contrast, N410 of the rat VDR stabilized, via backbone contacts, the interaction between helices 11 and 12. This results in TEI-9647 becoming a weak agonist in this organism.

Introduction

The nuclear receptor (NR) for the seco-steroid 1α,25$(OH)_2D_3$, VDR, is one of the 11 classic endocrine members of the NR superfamily that bind their respective ligands with high affinity (K_d value of 1 nM or lower) [1]. 1α,25$(OH)_2D_3$ is a key player in calcium homeostasis and bone mineralization [2] and also has antiproliferative and prodifferentiational effects on various cell types [3]. Like all NRs, VDR has a highly conserved DNA binding domain and a ligand binding domain (LBD) which is less conserved among members of this protein family. The LBD is formed by 12 α helices, and its overall architecture is similar in all NRs [4]. VDR, acting preferentially as a heterodimer with the retinoid X receptor (RXR), recognizes specific DNA sequences in promoter regions of 1α,25$(OH)_2D_3$ target genes, referred to as 1α,25$(OH)_2D_3$ response elements (VDREs) [5]. Over 3000 synthetic analogs of the natural hormone 1α,25$(OH)_2D_3$ have been synthesized. Most of these ligands are believed to interact with the VDR-RXR-VDRE complex. The central element of this molecular switch is the VDR-LBD [6], which can be stabilized by a 1α,25$(OH)_2D_3$ analog either in its agonistic, inverse agonistic, or antagonistic conformation. The stabilization of the agonistic conformation of the VDR-LBD is achieved by the repositioning of its most carboxy-terminal α helix (helix 12). In detail, this is achieved by a hydrogen bond between the C25-hydroxyl group of 1α,25$(OH)_2D_3$ and H397 of helix 11 of the receptor [7] and is supported by an additional, less important hydrogen bond with H305 [8]. In the presence of agonist, H397 is able to form van der Waals contacts with F422 of helix 12. This keeps helix 12 in a position that is optimal for the formation of the charge clamp between E420 (helix 12) and K246 (helix 3) and permits the binding of the LXXLL NR interaction domain of coactivator (CoA) proteins into a hydrophobic cleft on the surface of the VDR-LBD [9]. These CoA proteins in turn contact and recruit other components of the basal transcriptional machinery, resulting in the enhanced transcription of 1α,25$(OH)_2D_3$ target genes [10].

Most VDR ligands synthesized to date act as agonists [11]. Notable exceptions to this are the two-side chain analog Gemini and some of its derivatives, which are conditional inverse agonists [12, 13]. Only two types of VDR antagonist are known [14]. These are the 25-carboxylic esters exemplified by ZK159222 [15] and ZK168281 [12] and the 26,23-lactone TEI-9647 [16–18]. ZK159222 and TEI-9647 were characterized as partial antagonists, whereas ZK168281 is a pure antagonist [14, 19]. ZK159222 and ZK168281 show a functional affinity to the VDR that is comparable to that of 1α,25$(OH)_2D_3$, while that of TEI-9647 is at least 10-fold lower [14]. Molecular dynamics (MD) simulations of the VDR-LBD complexed with ZK159222 and ZK168281 suggest that the difference in the effects of these compounds arises from a more drastic displacement of helix 12 by ZK168281 than by ZK159222 [19]. In this antagonistic conformation, the interaction of the receptor LBD with CoAs is abolished or at least significantly reduced.

Selective antagonism as exhibited by TEI-9647, ZK159222, or the synthetic estrogen receptor ligands tamoxifen and raloxifene appears to be a complex phenomenon that arises through the interplay of a number of factors, such as differential ligand effects on the transactivation of the NR, the type of cofactor recruited, as well as cell and promoter contexts. For example, the antagonistic function of ZK159222 was shown to depend on the cell-specific ratio between VDR and RXR proteins [20]. So far, the partial antagonism of TEI-9647 has been explained by a reduced interaction of VDR with RXR and/or the CoA SRC-1 [18]. An alternative explanation involving covalent binding of this ligand to VDR has been excluded in a separate study [21]. This antagonism displays species-specific differences and was shown to be more potent in human osteosarcoma and promyelocytic leukemia cells [16–18]. In contrast to this, in a rat in vivo model, the action of TEI-9647 could not convincingly be distinguished from that of a weak VDR agonist [22].

In this study, we aimed to reveal the specific mechanisms of TEI-9647 action by using these species-specific differences. We found that the bulky lactone ring of this compound disturbs the exact positioning of helix 12 and therefore blocks the interaction with CoA proteins. Furthermore, in rat cells, we find that the residual

*Correspondence: carlberg@messi.uku.fi
[3]These authors contributed equally to this work.

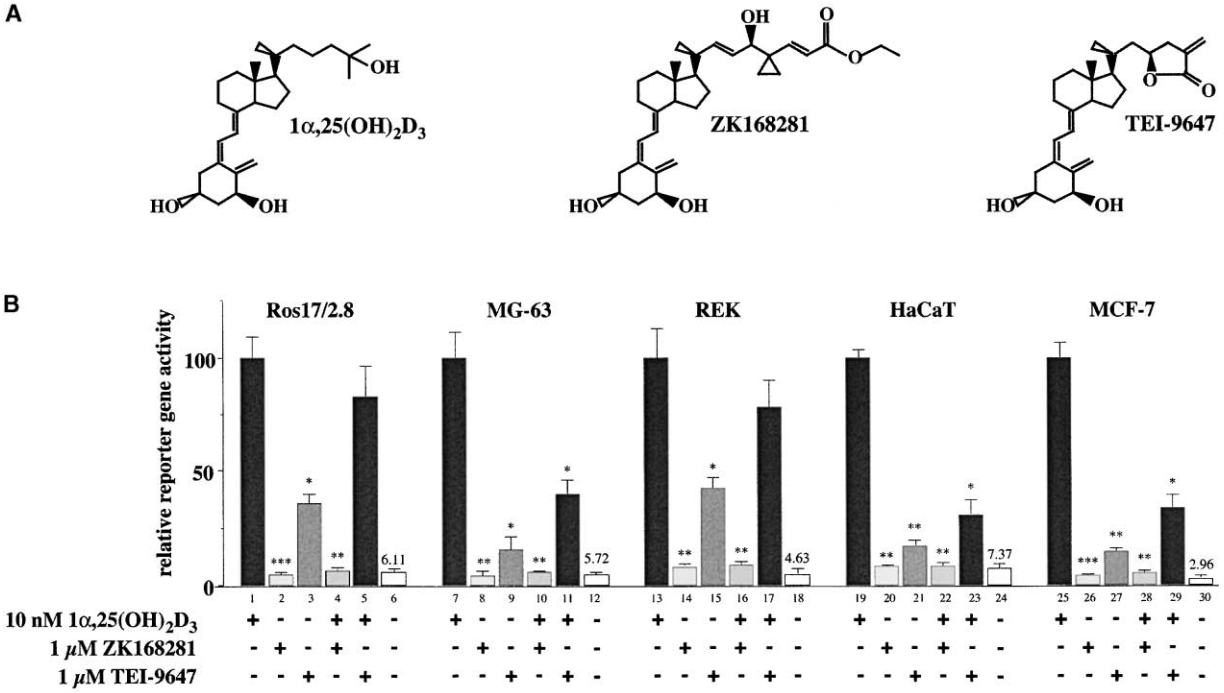

Figure 1. Species-Specific Differences in the Functional Profile of VDR Antagonists

The two-dimensional structures of $1\alpha,25(OH)_2D_3$, ZK168281, and TEI-9647 are shown (A). Luciferase reporter gene assays were performed on extracts from Ros17/2.8 (rat osteosarcoma), MG-63 (human osteosarcoma), REK (rat epidermal keratinocytes), HaCaT (human immortalized keratinocytes), and MCF-7 (human breast cancer) cells that were transfected by a reporter gene construct driven by four copies of the rat ANF DR3-type VDRE (B). Cells were treated for 16 hr with indicated concentrations of $1\alpha,25(OH)_2D_3$, ZK168281, or TEI-9647 alone and in combination. For each condition, luciferase activity was calculated in comparison to induction with the natural agonist. Columns represent the mean of triplicates, and the bars indicate standard deviation. The numbers above the solvent values indicate the relative basal activity. A two-tailed, paired Student's t test was performed, and p values were calculated in reference to maximal stimulation with $1\alpha,25(OH)_2D_3$ (*$p < 0.05$, **$p < 0.01$, ***$p < 0.001$).

agonistic activity of TEI-9647 was higher than that observed in human cells. We suggest that this is because the rodent-specific amino acids S403 and N410 display more and stronger interactions with TEI-9647 than C403 and C410 in humans. This results in a loss of the antagonist function of TEI-9647 in rodents.

Results and Discussion

The functional profile of the VDR antagonists ZK168281 and TEI-9647 were compared in Ros17/2.8 (rat osteosarcoma), MG-63 (human osteosarcoma), REK (rat epidermal keratinocytes), HaCaT (human immortalized keratinocytes), and MCF-7 (human breast cancer) cells. For this purpose, native VDR activity was assayed in the presence of the appropriate ligand using a luciferase reporter gene construct driven by four copies of a direct repeat (DR)3-type VDRE derived from the rat atrial natriuretic factor (ANF) gene. This construct was transiently transfected into the five cell lines, and the relative luciferase activity was determined after overnight stimulation in the presence of the appropriate ligand (Figure 1). In all cellular systems, ZK168281 was shown to have insignificant agonistic activity (lanes 2, 8, 14, 20, and 26). In combination with the natural agonist (lanes 4, 10, 16, 22, and 28), this ligand suppresses the natural ligand's inductive effect to a level which is comparable to that of solvent-treated cells. In contrast, at the same concentration (1 μM), TEI-9647 showed significant residual agonistic activity (lanes 3, 9, 15, 21, and 27), which was higher in rat (41%–45% of 10 nM $1\alpha,25(OH)_2D_3$) than in human (12%–15%) cells. The maximal induction of reporter gene activity through the natural agonist (lanes 1, 7, 13, 19, and 25) could be significantly reduced by a 100-fold molar excess of TEI-9647 in human cells (34%–39%, lanes 11, 23, and 29) but not in rat cells (78%–81%, lanes 5 and 17). Remarkably, the five cell lines differ in their relative basal activity and therefore their maximal inducibility by $1\alpha,25(OH)_2D_3$. For example, in Ros17/2.8 cells (lane 6) the basal activity was more than two times higher than in MCF-7 cells (lane 30). Taken together, the data indicate that TEI-9647 is a partial antagonist only in human cellular models but not in rat cells. In contrast, ZK168281 is a pure antagonist in both species.

The observation of the species-specific difference in the functional profile of TEI-9647 led us to hypothesize that it may be caused by amino acid differences in the VDR of rodent and human. The amino acid sequences of whole mouse and rat VDR are 96% identical, whereas the identities of both rodent VDRs with human VDR is 88%. However, only two amino acids differ between human and rodent VDR in the region close to the ligand binding pocket and helix 12. These differences occur

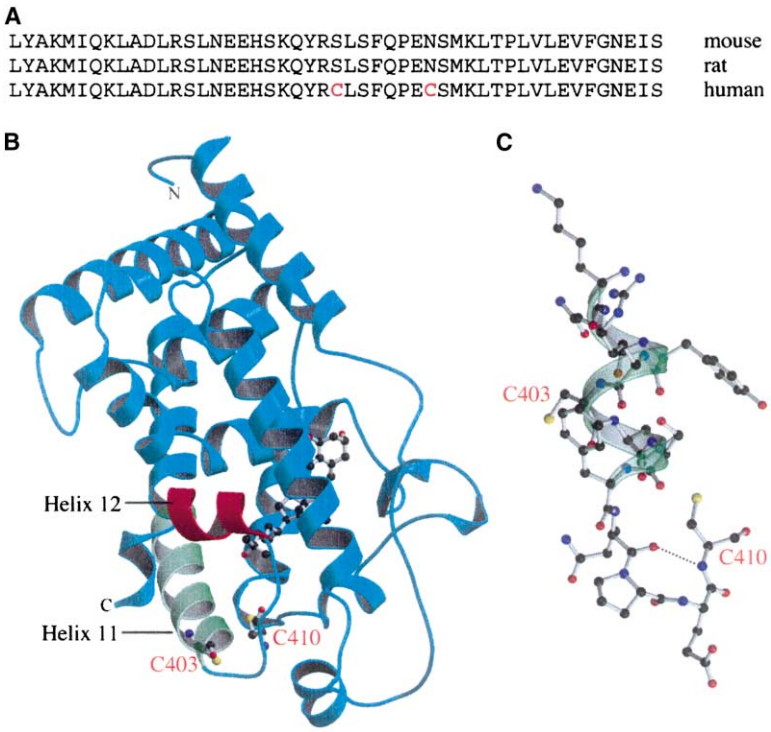

Figure 2. Differences between Rodent and Human VDR

Amino acid alignment of the C termini of mouse, rat, and human VDR (A). The only differences, C403 and C410 in human VDR, are highlighted (B). View of the whole LBD of human VDR complexed with $1\alpha,25(OH)_2D_3$. The α helices are represented by ribbons of C_α atoms (helix 11 in green and helix 12 in red), and only the side chains of C403 and C410 are shown. Detailed view on C403 in helix 11 and C410 in the loop to helix 12 in human VDR (C). Dashed lines indicate the interactions of C410. The average structures were collected from the last 500 ps of 6 ns MD simulations at 300 K.

at positions 403 and 410, respectively (Figure 2A). The rodent receptors both carry a serine and an asparagine residue at these positions, whereas the human VDR has two cysteines at positions 403 and 410, respectively. For MD simulations of the human VDR, initial coordinates were obtained from the X-ray crystal structure of the human VDR LBD-$1\alpha,25(OH)_2D_3$ complex [7], and the missing amino acid residues (positions 118, 119, 375–377, and 424–427) were modeled [19]. The simulations were performed for 6 ns, and the locations of C403 and C410 were found to be at the C terminus of helix 11 and at a hinge position in the loop between helices 11 and 12, respectively (Figure 2B). A detailed view of this area of the human VDR-LBD shows that C410 makes a single contact with its peptide bond nitrogen to the carbonyl group of P408 and has in this way a minor contribution to the orientation of the loop between helices 11 and 12 (Figure 2C). C403 is rather close to helix 12 (not shown in Figure 2C).

In order to test our hypothesis about the critical role of C403 and C410 in the function of TEI-9647 as a VDR antagonist, human VDR was mutated stepwise at both positions to serine and asparagine, respectively. The antagonistic profile of ZK168281 and TEI-9647 was tested in MCF-7 cells, which were overexpressing VDR_{wt}, VDR_{C403S}, VDR_{C410N}, and $VDR_{C430S/C410N}$ (Figure 3). The profile of VDR_{wt}-overexpressing MCF-7 cells (Figure 3A, lanes 1–6) resembled that of endogenous VDR expression (Figure 1, lanes 25–32), and the ligands ZK168281 and TEI-9647 behaved as a pure antagonist and a partial antagonist, respectively. The mutagenesis of VDR at positions 403 and 410 had virtually no effect on the antagonistic action of ZK168281 (Figure 3A, compare lanes 2, 8, 14, and 20 and lanes 4, 10, 16, and 22). In contrast, the single mutations C403S and C410N slightly, and the double mutation C403S/C410N significantly, increased the agonistic activity of TEI-9647 (compare lanes 3, 9, 15, and 21). The relative basal activity (compare lanes 6, 12, 18, and 24) significantly increased in the same order. Therefore, the mutagenesis of VDR has only minor effects on the absolute agonistic activity of TEI-9647. In VDR_{wt}- and VDR_{C403S}-overexpressing cells (lanes 5 and 11), TEI-9647 still showed some partial antagonistic action, which was lost in VDR_{C410N}- and $VDR_{C430S/C410N}$-overexpressing cells (lanes 17 and 23). Interestingly, the profile of $VDR_{C430S/C410N}$-overexpressing cells (lanes 19–24) was found to be similar to that of the rat cell lines Ros17/2.8 and REK (Figure 1, lanes 1–6 and 13–18). This suggests that, in rodents, TEI-9647 cannot act as an antagonist because S403 and N410 in rat VDR provide the receptor with a higher basal activity than C403 and C410 in human VDR. However, this seems not to affect the antagonistic function of ZK168281. We compared the agonistic profile of TEI-9647 and $1\alpha,25(OH)_2D_3$ on human VDR_{wt} and $VDR_{C430S/C410N}$ (Figure 3B) and found EC_{50} values of 3–4 nM for the natural hormone and 21–24 nM for TEI-9647. We conclude from this that there was no significant effect of the mutagenesis on the functional affinity of the receptor. This comparison demonstrated that the double mutation reduced the inducibility by $1\alpha,25(OH)_2D_3$, but not by TEI-9647, so that at the maximal concentration used, TEI-9647 reached approximately 40% of the agonistic activity of the natural hormone.

To further understand the role of positions 403 and 410 in the antagonistic versus the agonistic action of TEI-9647, supershift assays were performed using in vitro translated wt and mutant VDR, RXR, the rat ANF DR3-type VDRE, and the bacterially expressed p160 CoA transcription intermediary factor (TIF)2 (Figure 4). The

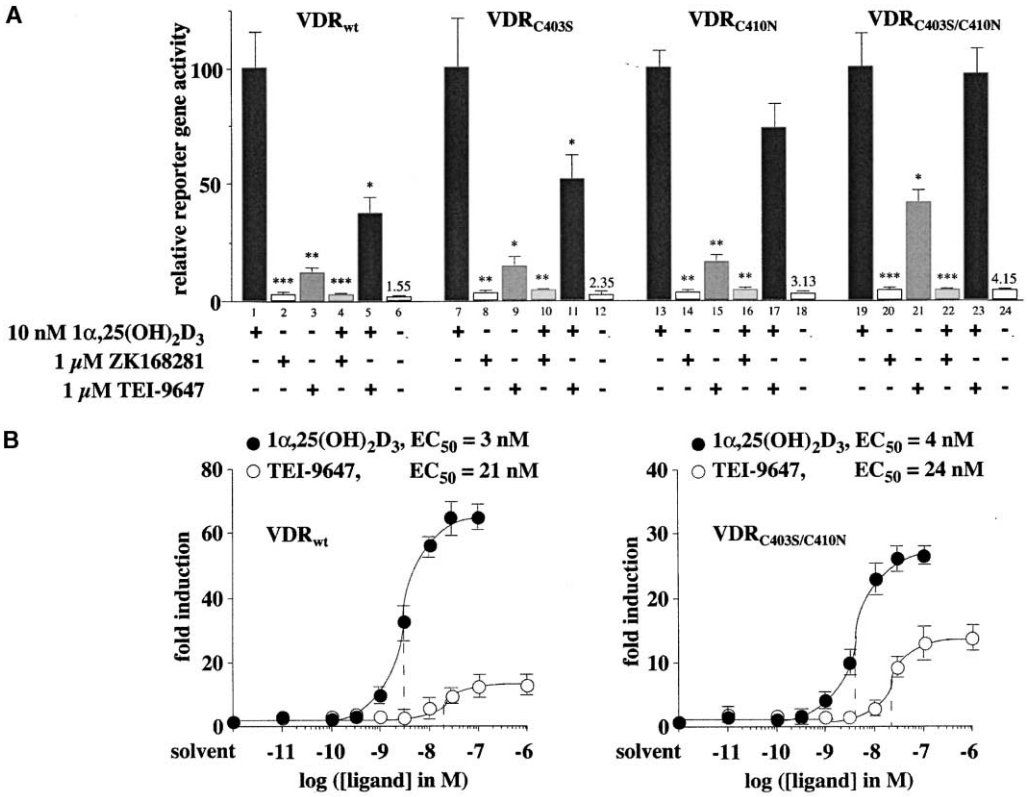

Figure 3. Substituting Rodent Amino Acids into the Human VDR Abolishes TEI-9647-Mediated Antagonism

Luciferase reporter gene assays were performed with extracts from MCF-7 human breast cancer cells that were transfected by a reporter gene construct driven by four copies of the rat ANF DR3-type VDRE and an expression vector for VDR$_{wt}$ or the indicated VDR mutant. Cells were treated for 16 hr with indicated concentrations of 1α,25(OH)$_2$D$_3$, ZK168281, or TEI-9647, alone and in combination (A) or with graded concentrations of 1α,25(OH)$_2$D$_3$ or TEI-9647 (B). For each condition, luciferase activity was calculated in comparison to induction with the natural agonist (A) or in reference to solvent control (B). Columns (A) and data points (B) represent the mean of triplicates, and the bars indicate standard deviation. The numbers above the solvent values (in [A]) indicate the relative basal activity. A two-tailed, paired Student's t test was performed, and p values were calculated in reference to maximal stimulation with 1α,25(OH)$_2$D$_3$ (*$p < 0.05$, **$p < 0.01$, ***$p < 0.001$).

natural ligand induced a supershift of VDR$_{wt}$, VDR$_{C403S}$, VDR$_{C410N}$, and VDR$_{C430S/C410N}$ with TIF2 (lanes 4, 12, 20, and 28), whereas in the presence of ZK168281 (lanes 6, 14, 22, and 30) or solvent (lanes 2, 10, 18, and 26), no complex with the CoA protein was detectable. TEI-9647 did not induce a shift with VDR$_{wt}$ (lane 8), only a very faint CoA complex with VDR$_{C403S}$ (lane 16), a slightly stronger interaction with VDR$_{C410N}$ (lane 24), and a dominant shift with VDR$_{C430S/C410N}$ (lane 32). No supershifted material was observed under any condition when GST-protein was used instead of the GST-TIF2 fusion protein. Taken together, mutating the cysteine residues of human VDR at positions 403 and 410 into those amino acids present at the orthologous positions in the rodent VDR increases the affinity of VDR for CoAs when the receptor binds TEI-9647. This is not observed for the pure VDR antagonist ZK168281. This parallels the observation of the functional assays (Figure 3) and indicates that TEI-9647 shifts from being an antagonist to a weak agonist when VDR is mutated at the two critical positions 403 and 410.

The loss of the antagonistic potential of TEI-9647 should also be reflected by a loss of the ligand-mediated stabilization of the antagonistic LBD conformation. To monitor possible changes in the ligand-dependent stabilization of VDR-LBD conformations, limited protease digestion assays, which report on the flexibility of the C-terminal of the VDR, were performed with VDR$_{wt}$, VDR$_{C403S}$, VDR$_{C410N}$, and VDR$_{C430S/C410N}$ (Figure 5). With VDR$_{wt}$, both ZK168281 and TEI-9647 stabilize a subpopulation of all VDR molecules in the antagonist-specific conformation c2 (lanes 3 and 4). Previously we have found that ZK168281 and TEI-9647 each stabilize slightly different antagonistic conformations [14]. As a control, 1α,25(OH)$_2$D$_3$ stabilized the agonistic conformation c1 and to a lower extent the inverse agonistic conformation c3 (lane 2), whereas in the presence of solvent, only a very low amount of the VDR input was stabilized in c1 and c3 (lane 1). The conformation profile of VDR$_{C410N}$ (lanes 9–12) resembled that of VDR$_{wt}$, where both TEI-9647 and ZK168281 acted as antagonists with this VDR mutant. In contrast, with VDR$_{C403S}$ and VDR$_{C430S/C410N}$, ZK168281 (lanes 7 and 15), but not TEI-9647 (lane 8 and 16), was able to stabilize the antagonistic conformation c2. This result indicates that TEI-9647 has lost its antagonistic potential. Since the limited protease digestion assay primarily reports the flexibility of the C terminus of the VDR, specifically C-terminal to the trypsin digestion site at R391, the loss of the antagonist-specific

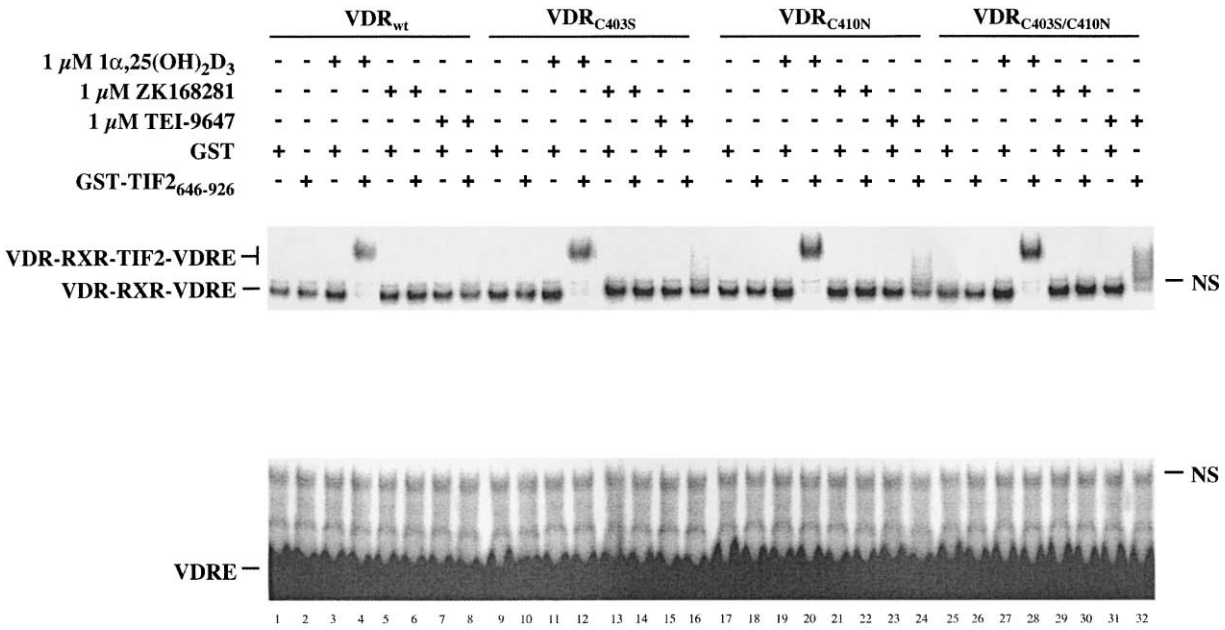

Figure 4. Ligand-Induced Cofactor Interaction Correlates with Action of VDR Antagonists

Supershift experiments were performed with heterodimers of in vitro translated VDR$_{wt}$ or its mutants with RXRα that were preincubated in the presence of bacterially expressed GST (as a control) or GST-TIF2$_{646-926}$ with 1 μM 1α,25(OH)$_2$D$_3$, 1 μM ZK168281, 1 μM TEI-9647, or solvent and the ^{32}P-labeled rat ANF DR3-type VDRE. Protein-DNA complexes were separated from free probe through 8% nondenaturing polyacrylamide gels. A representative experiment is shown. NS indicates nonspecific complexes.

conformation reflects a looser packing of the receptor in the area of the second trypsin digestion site at R402. We suggest that this occurs because of more flexiblity at the end of helix 11, where S403 is located. Therefore, the results of the limited protease digestion assay indicate that the exchange of a sulfhydryl for a hydroxyl group increases the electronegativity at position 403, and this in turn reduces the flexibility of helix 12. In this way, the mutation C403S also contributes to the increased constitutive activity of the VDR (see Figure 3). In summary, C403, but not C410, appears to be critical for the stabilization of the antagonistic conformation of VDR by TEI-9647, whereas its stabilization by ZK168281 was not influenced by either of these two cysteines.

Further MD simulations (6 ns) were performed with VDR$_{wt}$ complexed with 1α,25(OH)$_2$D$_3$, ZK168281 and TEI-9647 and with VDR$_{C430S/C410N}$ bound by TEI-9647 in order to understand the basis of the effects of these ligands have on VDR (Figure 6). The simulations were calculated with the whole VDR-LBD, but only the ligand and helices 11 and 12 are shown. The 25-hydroxyl group of the natural ligand contacts H397 in helix 11, which in turn stabilizes the position of helix 12 via an interaction with F422 (Figure 6A). This keeps the negatively charged E420 of helix 12 at an optimal distance (19 Å) from the positively charged K246 of helix 3. This enables the formation of the charge clamp that stabilizes the LBD-CoA interaction (data not shown; compare [19]). In contrast, the extended, rigid side chain of ZK168281 disturbs the interaction between H397 and F422 and thus the stable positioning of helix 12 (Figure 6B). This blocks the ability to interact with CoA protein and explains the pure antagonistic profile of ZK168281 [14, 19]. The lactone ring of TEI-9647 is more bulky than the end of the side chain of the natural hormone and cannot interact effectively with H397 and H305. Moreover, the carbonyl group of the lactone ring cannot interact directly with F422. These observations indicate that steric hindrance plays a role in this ligand's antagonstic behavior. However, TEI-9647 lacks an extended side chain and disturbs helix 12 less than ZK168281 (Figure 6C). In fact, the disturbance of helix 12 by TEI-9647 is so weak that it can be counterbalanced by backbone contacts of N410 in VDR$_{C430S/C410N}$ with P408 and L404 (Figure 6D). Therefore, in rodent VDRs the backbone contacts of their loop amino acid N410 stabilize the helix 11-helix 12 interaction (Figure 6E) so that the LBD of rodent VDR binds CoA proteins even in the presence of TEI-9647. This supports the finding that TEI-9647 behaves as a weak agonist rather than as an antagonist in rodents.

The differences in the structures of the complexes of VDR$_{wt}$ and VDR$_{C430S/C410N}$ with TEI-9647 are better illustrated when the variation of the backbone root-mean-square deviation (rmsd) of amino acids 393–422 and the distance between the C$_\alpha$ atoms of T415 and F422 are monitored over the whole MD simulation period of 6 ns (Figure 7). The rmsd can be used to indicate the mobility of helices 11 and 12 and is inversely proportional to the stability of helix 12. After 2.5 ns of MD simulation, the rmsd of the VDR$_{wt}$-TEI-9647 complex was significantly higher than that of the complexes of VDR$_{wt}$ with 1α,25(OH)$_2$D$_3$ and of VDR$_{C430S/C410N}$ with 1α,25(OH)$_2$D$_3$ or TEI-9647 (Figure 7A). Interestingly, the latter three LBD-ligand complexes have the same average rmsd, indicating their comparable ability to stabilize the interaction

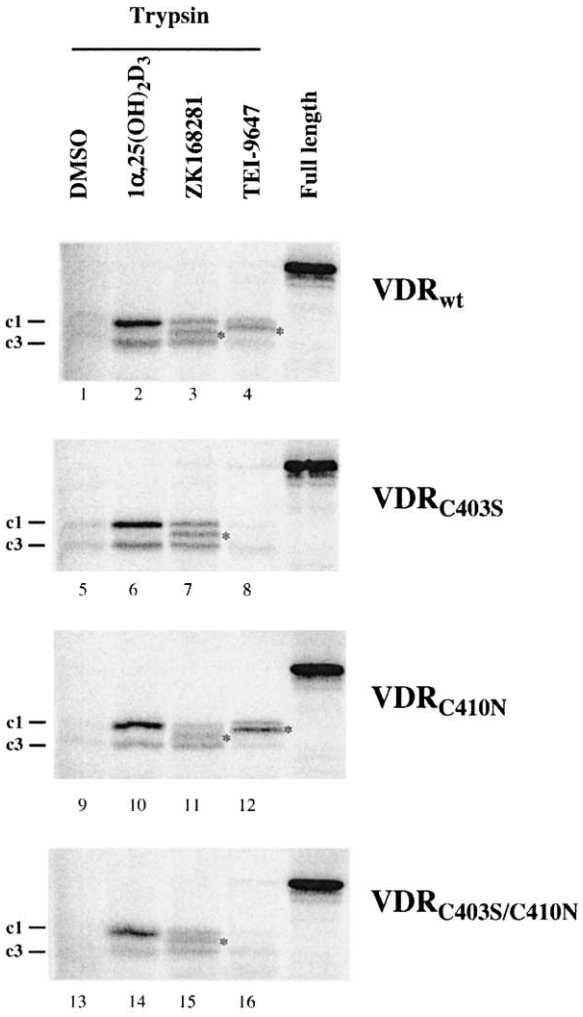

Figure 5. Stabilization of Agonistic and Antagonistic VDR Conformations

Limited protease digestion assays were performed by preincubating in vitro translated ^{35}S-labeled wild-type or mutant VDR with DMSO (as solvent control) or saturating concentrations (10 μM) of 1α,25(OH)$_2$D$_3$, ZK168281, or TEI-9647. After digestion with trypsin, the ligand-stabilized VDR conformations c1 (active) and c3 (silent) were electrophoresed through 15% SDS-polyacrylamide gels. The antagonist-specific conformation c2 is indicated by an asterisk. Representative experiments are shown.

with CoA proteins. The peak after 4 ns of the simulation of VDR$_{wt}$ with 1α,25(OH)$_2$D$_3$ is due to a transient conformational change in the loop region (residues 407–414) between helices 12 and 11. The distance between the C$_\alpha$ atoms of T415 and F422 measures the length of helix 12 (Figure 7B). An increased length of helix 12 is a sign of greater flexibility and is inversely proportional to the probability of an interaction with a CoA proteins. In this view of the structures, the VDR$_{wt}$-TEI-9647 complex was shown after 2 ns of simulations to have a significantly longer and more flexible helix 12 than the complexes of VDR$_{wt}$ with 1α,25(OH)$_2$D$_3$ and of VDR$_{C430S/C410N}$ with 1α, 25(OH)$_2$D$_3$ or TEI-9647. Again, the latter two LBD-ligand complexes appeared to be identical and had the same average length of helix 12 (10.7–10.9 Å, which is close to 10.8 Å in the X-ray crystal structure of the VDR$_{wt}$-1α,25(OH)$_2$D$_3$-complex [7]).

The observation of a significant difference in the constitutive activity of human and rodent VDR was unexpected. In human VDR, C410 forms only one hydrogen bond with the backbone of helix 11, whereas in rodents N410 makes two additional contacts. In addition, the increased interaction strength of S403 compared to C403 supports the effect of N410 in stabilizing helix 12 for an interaction with helix 11. This provides human VDR$_{C403S/C410N}$ with a more than 2-fold increased ligand-independent constitutive activity over VDR$_{wt}$ and perfectly mimics the reduced agonist inducibility of the rat versus human wild-type VDR. Although the inducibility of endogenous rat VDR or overexpressed VDR$_{C403S/C410N}$ by 1α,25(OH)$_2$D$_3$ is reduced, the absolute induction of the receptor by TEI-9647 is not decreased. This leads to an apparent doubling of the relative agonistic action of this ligand. This results in a loss of the antagonistic action of the compound when combined with the rather low receptor binding affinity of TEI-9647. Chemical modifications of TEI-9647, in particular at its 2α position, significantly increase the VDR binding affinity [23, 24]. These compounds have the potential to act even in rodents as partial antagonists. The molecular mechanism of the antagonistic action of TEI-9647 in human cells is not as obvious as that of the 25-carboxylic ester ZK168281, but the bulky lactone ring of TEI-9647 disturbs the H397-F422 interaction. This destabilizes the position of helix 12, induces flexibility to the helix, and makes a stable interaction of the LBD with CoA proteins unlikely. However, TEI-9647 derivatives with rather bulky and/or extended substitutents at their 2α position [23, 24] cannot sit as deep in the ligand binding pocket as an unsubstituted ligand. This decreases the distance between the carbonyl group of the lactone ring and F422 and provides the respective compounds with a higher antagonistic potential than the parental compound.

A mixed agonist/antagonist profile, such as reported here for TEI-9647 on rodent and human VDR, was also observed for 5,11-*cis*-diethyl-5,6,11,12-tetra-hydrochysene-2,8-diol on estrogen receptor (ER) α and β [25]. With ERα this compound acts as an agonist, whereas on ERβ it functions as antagonist. This property was called passive antagonism. In this respect, TEI-9647 could also be referred to as a passive antagonist.

Significance

Agonism and antagonism of NR ligands are closely related processes. Both types of ligand bind to the same site in the ligand binding pocket, but agonists stabilize the position of helix 12, whereas antagonists prevent this stabilization. TEI-9647 binds the ligand binding pocket of the VDR with lower affinity than the natural agonist and acts in human cells as a partial antagonist. In rat cells, the residual agonistic activity of TEI-9647 is significantly higher than in human cells, because the rodent-specific amino acids S403 and N410 display more and stronger interactions than C403 and C410 in humans. The bulky lactone ring of TEI-9647 disturbs the exact positioning of helix 12,

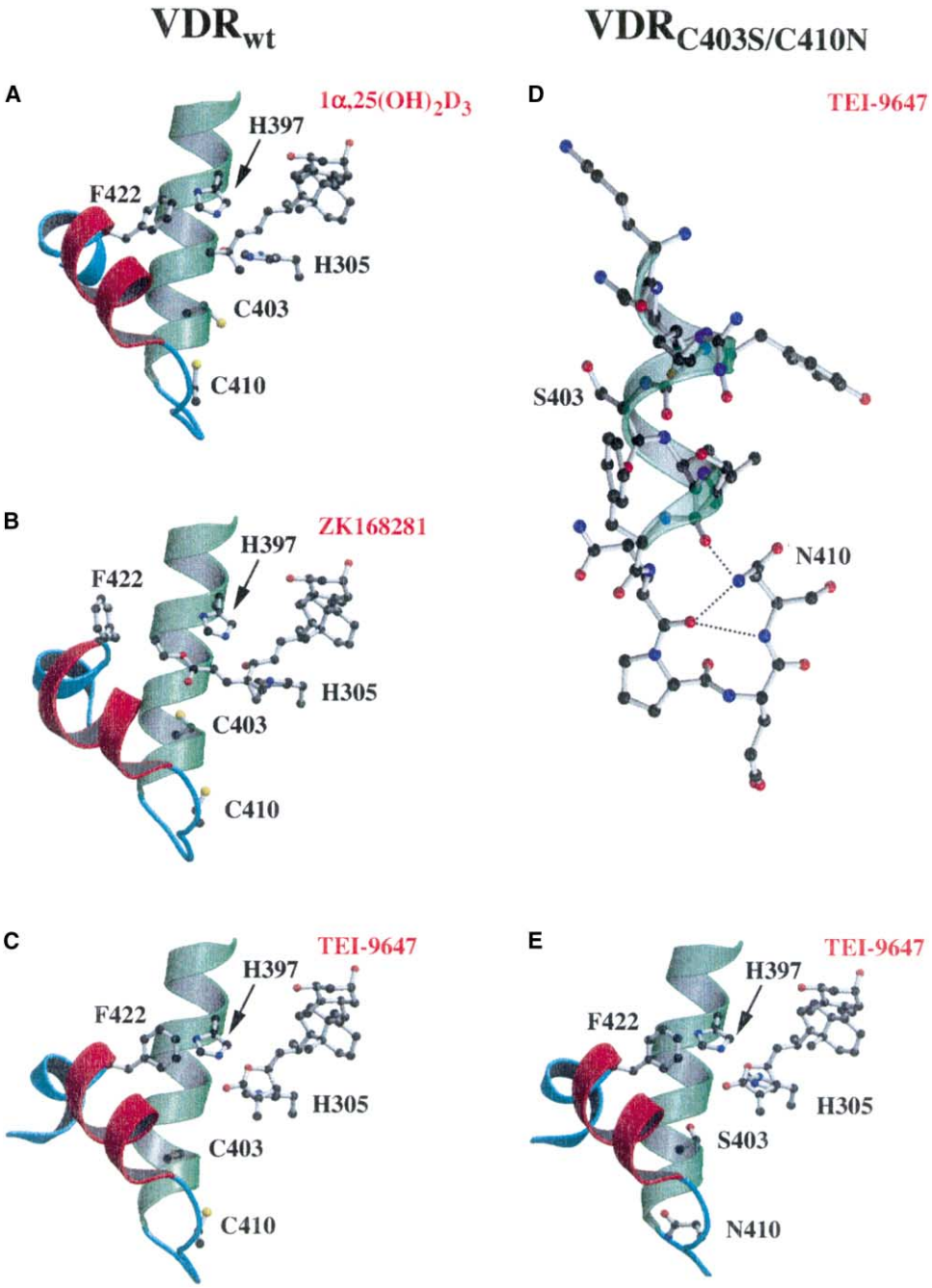

Figure 6. MD Simulations of LBD-Ligand Complexes

Average structures of VDR_{wt} (A–C) or $VDR_{C403/C410}$ (D and E) complexed with $1\alpha,25(OH)_2D_3$ (A), ZK168281 (B), or TEI-9647 (C–E) were collected from the last 500 ps of 6 ns MD simulations at 300 K. Please note that the coordinates for the VDR-ZK168281 complex were taken from our previous publication [19]. The relative position of the ligand in relation to helices 11 and 12 is shown. Detailed view on S403 in helix 11 and N410 the loop to helix 12 in $VDR_{C403/C410}$ (D). Dashed lines indicate the backbone interactions of N410 with P408 and L404.

which results in a decreased interaction with CoA proteins. However, the displacement of helix 12 by TEI-9647 is much weaker than that by the pure antagonist ZK168281, so that only the 26,23-lactone but not the 25-carboxylic ester is affected by the increased interaction potential of S403 and N410 in rodent VDR. This results in a loss of the antagonist function of TEI-9647 in rodents. However, derivatives of TEI-9647 with increased VDR binding affinity, which in parallel cause more disturbance to helix 12, have the potential to be effective VDR antagonists.

Experimental Procedures

Compounds

The natural hormone $1\alpha,25(OH)_2D_3$ was a kind gift from Dr. Lise Binderup (LEO Pharma, Ballerup, Denmark), its 25-carboxylic ester

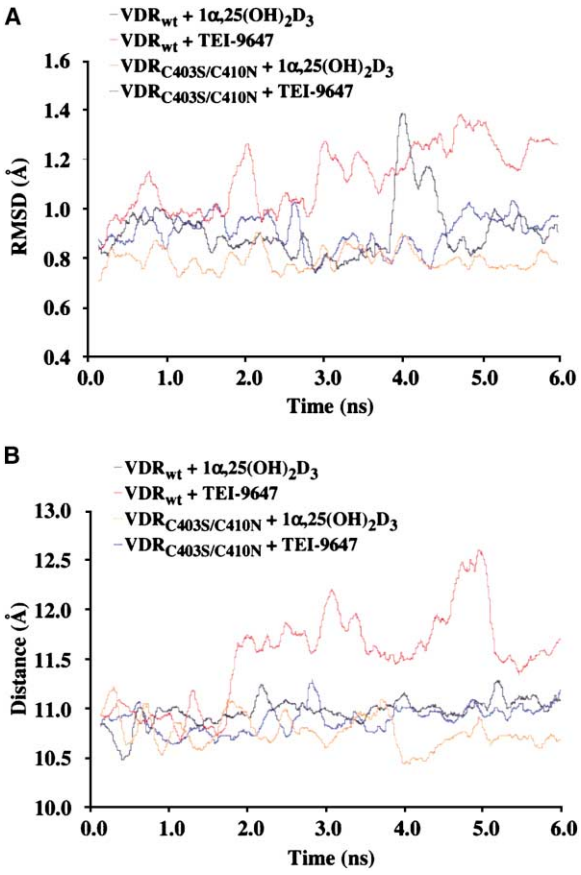

Figure 7. Critical Changes of the LBD-TEI-9647 Complex

During 6.0 ns MD simulations, the backbone (N, C_α, C, O) rmsd of residues 393–422 (A) and the distance between the C_α atoms of T415 and F422 (B) were compared for the complexes of VDR_{wt} and $VDR_{C403/C410}$ with 1α,25(OH)$_2$D$_3$ or TEI-9647. The latter distance measures the length of helix 12 and is 10.8 Å in the X-ray structure of the VDR_{wt}-1α,25(OH)$_2$D$_3$-complex [7].

analog ZK168281 [12] was provided by Dr. Andreas Steinmeyer (Schering AG, Berlin, Germany), and the 26,23-lactone analog TEI-9647 [16] was a gift from Dr. Seiichi Ishizuka (Teijin Institute for Bio-Medical Research, Tokyo, Japan). All compounds were dissolved in 2-propanol; further dilutions were made in DMSO (for in vitro assays) or in ethanol (for cell culture assays).

DNA Constructs

The full-length cDNAs for human VDR [26] and human RXRα [27] were subcloned into the SV40 promoter-driven pSG5 expression vector (Stratagene, La Jolla, CA). The same constructs were used for both T_7 RNA polymerase-driven in vitro transcription/translation of the respective cDNAs and for viral promoter-driven overexpression of the respective proteins in mammalian cells. The point mutants of VDR were generated using the QuikChange Point Mutagenesis Kit (Stratagene) and confirmed by sequencing. The luciferase reporter gene was driven by four copies of the rat ANF DR3-type binding site (core sequence AG**AGGTCA**TGA**AGGACA**) fused to the *tk* promoter. The NR interaction domain of human TIF2 (spanning amino acids 646 to 926) [28] was subcloned into the GST fusion vector pGEX (Amersham-Pharmacia, Uppsala, Sweden).

Transfection and Luciferase Reporter Gene Assays

Ros17/2.8 (rat osteosarcoma), MG-63 (human osteosarcoma), REK (rat epidermal keratinocytes), HaCaT (human immortalized keratinocytes), and MCF-7 (human breast cancer) cells were seeded into 6-well plates (10^5 cells/ml) and grown overnight in phenol red-free DMEM supplemented with 5% charcoal-treated fetal bovine serum. Liposomes were formed by incubating 1 μg of the reporter plasmid and, in indicated cases, 1 μg of expression vector for VDR or its mutants with 10 μg N-[1-(2,3-Dioleoyloxy)propyl]-N,N,N-trimethylammonium methylsulfate (DOTAP, Roth, Karlsruhe, Germany) for 15 min at room temperature in a total volume of 100 μl. After dilution with 900 μl phenol red-free DMEM, the liposomes were added to the cells. Phenol red-free DMEM supplemented with 15% charcoal-treated fetal bovine serum (500 μl) was added 4 hr after transfection. At this time, VDR ligands at the indicated concentrations were also added. The cells were lysed 16 hr after onset of stimulation using the reporter gene lysis buffer (Roche Diagnostics, Mannheim, Germany), and the constant light signal luciferase reporter gene assay was performed as recommended by the supplier (Canberra-Packard, Groningen, The Netherlands). The luciferase activities were normalized with respect to protein concentration, and relative values were calculated relative to that treated with the natural agonist.

Protein Production and Supershift Assay

In vitro translated wild-type or mutated human VDR and human RXRα proteins were generated by coupled in vitro transcription/translation using rabbit reticulocyte lysate as recommended by the supplier (Promega, Madison, WI). Protein batches were quantified by test-translations in the presence of [^{35}S]methionine. The specific concentrations of the receptor proteins were adjusted to approximately 4 ng/μl after taking the individual number of methionine residues per protein into account. Bacterial overexpression of GST-$TIF2_{646-926}$ or GST alone (as a control) was obtained from the *E. coli* BL21(DE3)pLysS strain (Stratagene) containing the respective expression plasmids. Overexpression was stimulated with 0.25 mM isopropyl-β-D-thio-galactopyranoside for 3 hr at 37°C, and the proteins were purified and immobilized on glutathione-Sepharose 4B beads (Amersham-Pharmacia) according to the manufacturer's protocol. Proteins were eluted in the presence of glutathione. For supershift assays, in vitro translated VDR-RXR heterodimers were incubated with saturating concentrations of 1α,25(OH)$_2$D$_3$ or its analogs for 15 min at room temperature in a total volume of 20 μl binding buffer (10 mM HEPES [pH 7.9], 1 mM DTT, 0.2 μg/μl poly(dI-C), and 5% glycerol). The buffer had been adjusted to 150 mM by addition of KCl. Then 3 μg of bacterially expressed GST or GST-$TIF2_{646-926}$ protein and 1 ng (approximately 50,000 cpm) of the ^{32}P-labeled rat ANF DR3-type VDRE were added, and incubation was continued for 20 min. Protein-DNA complexes were resolved through 8% nondenaturing polyacrylamide gels in 0.5× TBE (45 mM Tris, 45 mM boric acid, 1 mM EDTA [pH 8.3]). The gels were dried, exposed to a Fuji MP2040S imager screen (Fuji, Tokyo, Japan), and monitored on a Fuji FLA3000 reader.

Limited Protease Digestion Assay

In vitro translated, ^{35}S-labeled VDR protein (2.5 μl) was incubated with the appropriate ligand for 15 min at room temperature in 10 μl 50 mM Tris-HCl (pH 7.9). Trypsin (Promega, final concentration 20 ng/μl) was then added, and the mixtures were further incubated for 15 min at room temperature. The digestion reactions were stopped by adding 10 μl protein gel loading buffer (0.25 M Tris [pH 6.8], 20% glycerol, 5% mercaptoethanol, 2% SDS, 0.025% bromophenol blue). The samples were denatured at 85°C for 3 min and electrophoresed through 15% SDS-polyacrylamide gels. The gels were dried, exposed to a Fuji MP2040S imager screen, and monitored on a Fuji FLA3000 reader.

MD Simulations

The initial coordinates for the MD simulations were obtained from the X-ray crystal structure of the VDR LBD-1α,25(OH)$_2$D$_3$ complex (Protein Data Bank code 1DB1) determined to 1.8 Å resolution [7]. The missing amino acid residues of the X-ray structure (residues 118, 119, 375–377, and 424–427) were built using the Quanta98 molecular modeling package (Molecular Simulations Inc., San Diego, CA). The four residues missing from the C terminus (424–427) were built in an α-helical conformation ($\phi = -57°$, $\psi = -47°$). The two VDR antagonists, ZK168281 and TEI-9647, were docked to the ligand binding site of LBD using the locally enhanced sampling

method, which is a mean-field technique providing the ability to focus on the interesting part of the system. Crystallographic water molecules were included in simulation systems. The side chains of the C403S/C410N double mutant LBD were built using the C_α and S_β atoms of the cysteines mutated. For the MD simulations, the protein-ligand complexes were solvated by 10,779 TIP3P water molecules in a periodic box of 69 $\times$ 61 $\times$ 87 Å. The water molecules of the complexes were first energy-minimized for 2000 steps, heated to 300 K in 10 ps, and equilibrated by 40 ps at a constant temperature of 300 K and pressure of 1 atm. The production simulations of 6 ns were then started. In the simulations, the electrostatics were treated using the particle-mesh Ewald method. A timestep of 1.5 fs was used, and bonds involving hydrogen atoms were constrained to their equilibrium lengths using the SHAKE algorithm. From the production simulations, structures were saved every 0.75 ps for analyses, which were done using the carnal and ptraj programs of the AMBER7.0 simulation package (University of California, San Francisco, CA). The simulations were done using the PMEMD 3.03 program (University of North Carolina-Chapel Hill, NC) and the Cornell et al. force field [29]. The parameters of the ligands were generated with the Antechamber suite of AMBER7.0 in conjunction with the general amber force field. The atomic point charges of the ligands were calculated with the two-stage RESP [30] fit at the HF/6-31G* level using ligand geometries optimized with the semiempirical PM3 method using the Gaussian98 program (Gaussian Inc., Pittsburgh, PA).

Acknowledgments

We thank Drs. Lise Binderup, Andreas Steinmeyer, and Seiichi Ishizuka for providing VDR ligands and Dr. Thomas W. Dunlop for critical reading of the manuscript. The Academy of Finland (grant 50319 to C.C. and grant 74097 to M.P.) supported this work.

Received: February 28, 2004
Revised: May 5, 2004
Accepted: May 25, 2004
Published: August 20, 2004

References

1. Chawla, A., Repa, J.J., Evans, R.M., and Mangelsdorf, D.J. (2001). Nuclear receptors and lipid physiology: opening the X-files. Science *294*, 1866–1870.
2. Suda, T., Ueno, Y., Fujii, K., and Shinki, T. (2003). Vitamin D and bone. J. Cell. Biochem. *88*, 259–266.
3. Mørk Hansen, C., Binderup, L., Hamberg, K.J., and Carlberg, C. (2001). Vitamin D and cancer: effects of 1,25(OH)$_2$D$_3$ and its analogs on growth control and tumorigenesis. Front. Biosci. *6*, D820–D848.
4. Andersin, T., Väisänen, S., and Carlberg, C. (2003). The critical role of carboxy-terminal amino acids in ligand-dependent and -independent transactivation of the constitutive androstane receptor. Mol. Endocrinol. *17*, 234–246.
5. Onate, S.A., Tsai, S.Y., Tsai, M.J., and O'Malley, B.W. (1995). Sequence and characterization of a coactivator for the steroid hormone receptor superfamily. Science *270*, 1354–1357.
6. Hörlein, A.J., Näär, A.M., Heinzel, T., Torchia, J., Gloss, B., Kurokawa, R., Ryan, A., Kamei, Y., Söderström, M., Glass, C.K., et al. (1995). Ligand-independent repression by the thyroid hormone receptor mediated by a nuclear receptor co-repressor. Nature *377*, 397–404.
7. Rochel, N., Wurtz, J.M., Mitschler, A., Klaholz, B., and Moras, D. (2000). Crystal structure of the nuclear receptor for vitamin D bound to its natural ligand. Mol. Cell *5*, 173–179.
8. Väisänen, S., Ryhänen, S., Saarela, J.T., Peräkylä, M., Andersin, T., and Maenpää, P.H. (2002). Structurally and functionally important amino acids of the agonistic conformation of the human vitamin D receptor. Mol. Pharmacol. *62*, 788–794.
9. Feng, W., Ribeiro, R.C.J., Wagner, R.L., Nguyen, H., Apriletti, J.A., Fletterick, R.J., Baxter, J.D., Kushner, P.J., and West, B.L. (1998). Hormone-dependent coactivator binding to a hydrophobic cleft on nuclear receptors. Science *280*, 1747–1749.
10. Freedman, L.P. (1999). Increasing the complexity of coactivation in nuclear receptor signaling. Cell *97*, 5–8.
11. Carlberg, C., and Mouriño, A. (2003). New vitamin D receptor ligands. Expert Opin. Ther. Patents *13*, 761–772.
12. Bury, Y., Steinmeyer, A., and Carlberg, C. (2000). Structure activity relationship of carboxylic ester antagonists of the vitamin D$_3$ receptor. Mol. Pharmacol. *58*, 1067–1074.
13. Macias-Gonzalez, M., Samenfeld, P., Perakyla, M., and Carlberg, C. (2003). Corepressor excess shifts the two-side chain vitamin D analog Gemini from an agonist to an inverse agonist of the vitamin D receptor. Mol. Endocrinol. *17*, 2028–2038.
14. Toell, A., Gonzalez, M.M., Ruf, D., Steinmeyer, A., Ishizuka, S., and Carlberg, C. (2001). Different molecular mechanisms of vitamin D$_3$ receptor antagonists. Mol. Pharmacol. *59*, 1478–1485.
15. Herdick, M., Steinmeyer, A., and Carlberg, C. (2000). Antagonistic action of a 25-carboxylic ester analogue of 1α,25-dihydroxyvitamin D$_3$ is mediated by a lack of ligand-induced vitamin D receptor interaction with coactivators. J. Biol. Chem. *275*, 16506–16512.
16. Miura, D., Manabe, K., Ozono, K., Saito, M., Gao, Q., Norman, A.W., and Ishizuka, S. (1999). Antagonistic action of novel 1α,25-dihydroxyvitamin D$_3$-26,23-lactone analogs on differentiation of human leukemia cells (HL-60) induced by 1α,25-dihydroxyvitamin D$_3$. J. Biol. Chem. *274*, 16392–16399.
17. Miura, D., Manabe, K., Gao, Q., Norman, A.W., and Ishizuka, S. (1999). 1α,25-dihydroxyvitamin D$_3$-26,23-lactone analogues antagonize differentiation of human leukemia cells (HL-60 cells) but not of human acute promyelocytic leukemia cells (NB4 cells). FEBS Lett. *460*, 297–302.
18. Ozono, K., Saiti, M., Miura, D., Michigami, T., Nakajima, S., and Ishizuka, S. (1999). Analysis of the molecular mechanism for the antagonistic action of a novel 1α,25-dihydroxyvitamin D$_3$ analogue toward vitamin D receptor function. J. Biol. Chem. *274*, 32376–32381.
19. Väisänen, S., Peräkylä, M., Kärkkäinen, J.I., Steinmeyer, A., and Carlberg, C. (2002). Critical role of helix 12 of the vitamin D$_3$ receptor for the partial agonism of carboxylic ester antagonists. J. Mol. Biol. *315*, 229–238.
20. Herdick, M., Steinmeyer, A., and Carlberg, C. (2000). Carboxylic ester antagonists of 1α,25-dihydroxyvitamin D$_3$ show cell-specific actions. Chem. Biol. *7*, 885–894.
21. Bula, C.M., Bishop, J.E., Ishizuka, S., and Norman, A.W. (2000). 25-Dehydro-1α-hydroxyvitamin D$_3$-26,23S-lactone antagonizes the nuclear vitamin D receptor by mediating a unique noncovalent conformational change. Mol. Endocrinol. *14*, 1788–1796.
22. Ishizuka, S., Miura, D., Ozono, K., Chokki, M., Mimura, H., and Norman, A.W. (2001). Antagonistic actions *in vivo* of (23S)-25-dehydro-1α-hydroxyvitamin D$_3$-26,23-lactone on calcium metabolism induced by 1α,25-dihydroxyvitamin D$_3$. Endocrinology *142*, 59–67.
23. Saito, N., Saito, H., Anzai, M., Yoshida, A., Fujishima, T., Takenouchi, K., Miura, D., Ishizuka, S., Takayama, H., and Kittaka, A. (2003). Dramatic enhancement of antagonistic activity on vitamin D receptor: a double functionalization of 1α-hydroxyvitamin D$_3$ 26,23-lactones. Org. Lett. *5*, 4859–4862.
24. Fujishima, T., Kojima, Y., Azumaya, I., Kittaka, A., and Takayama, H. (2003). Design and synthesis of potent vitamin D receptor antagonists with A-ring modifications: remarkable effects of 2α-methyl introduction on antagonistic activity. Bioorg. Med. Chem. *11*, 3621–3631.
25. Shiau, A.K., Barstad, D., Radek, J.T., Meyers, M.J., Nettles, K.W., Katzenellenbogen, B.S., Katzenellenbogen, J.A., Agard, D.A., and Greene, G.L. (2002). Structural characterization of a subtype-selective ligand reveals a novel mode of estrogen receptor antagonism. Nat. Struct. Biol. *9*, 359–364.
26. Carlberg, C., Bendik, I., Wyss, A., Meier, E., Sturzenbecker, L.J., Grippo, J.F., and Hunziker, W. (1993). Two nuclear signalling pathways for vitamin D. Nature *361*, 657–660.
27. Levin, A.A., Sturzenbecker, L.J., Kazmer, S., Bosakowski, T., Huselton, C., Allenby, G., Speck, J., Kratzeisen, C., Rosenberger, M., Lovey, A., et al. (1992). 9-*Cis* retinoic acid stereoisomer binds and activates the nuclear receptor RXRα. Nature *355*, 359–361.

28. Voegel, J.J., Heine, M.J.S., Zechel, C., Chambon, P., and Gronemeyer, H. (1996). TIF2, a 160 kDa transcriptional mediator for the ligand-dependent activation function AF-2 of nuclear receptors. EMBO J. *15*, 3667–3675.
29. Cornell, W.D., Cieplak, P., Bayly, C.I., Gould, I., Merz, K.M., Ferguson, D., Spellmeyer, D.C., Fox, T., Caldwell, J.W., and Kollman, P.A. (1995). A second generation force field for the simulation of proteins, nucleic acids, and organic molecules. J. Am. Chem. Soc. *117*, 5179–5197.
30. Bayly, C.I., Cieplak, P., Cornell, W.D., and Kollman, P.A. (1993). A well-behaved electrostatic potential based method using charge restraints for deriving atomic charges: the RESP model. J. Phys. Chem. *97*, 10269–10280.